Annals of Biomedical Engineering, Vol. 28, pp. 524–532, 2000
Printed in the USA.

0090-6964/2000/28(5)/524/9/$15.00

An *In Vitro* Study of the Hinge and Near-Field Forward Flow Dynamics of the St. Jude Medical® Regent™ Bileaflet Mechanical Heart Valve

JEFFREY T. ELLIS,[1] BRANDON R. TRAVIS,[2] and AJIT P. YOGANATHAN[3]

[1]School of Mechanical Engineering, [2]School of Chemical Engineering, and
[3]School of Biomedical Engineering, Georgia Institute of Technology, Atlanta, GA

(Received 11 August 1999; accepted 21 April 2000)

Abstract—The most widely implanted prosthetic valve is the mechanical bileaflet. Recent clinical experiences suggest that some designs are more prone to thromboembolic episodes than others. This study evaluated the hinge flow and near-field forward flow of the new St. Jude Medical® Regent™ bileaflet mechanical heart valve. Laser Doppler velocimetry measurements were conducted within the hinge and near-field forward flow regions of the Regent™ valve. These pulsatile flow velocity measurements were animated in time to visualize the flow fields throughout the cardiac cycle. During forward flow, a recirculation region developed in the inflow pocket of the Regent™ hinge but was subsequently abolished by strong backflow during valve closure. Leakage velocities in the hinge region reached 0.72 m/s and Reynolds shear stresses reached 2,600 dyn/cm^2. Velocities in the near-field region were highest in the lateral orifice jet, reaching 2.1 m/s. Small regions of separated flow were observed adjacent to the hinge region. Leaflet motion through the Regent™ hinge creates a washout pattern which restricts the persistence of stagnation zones in its hinge. Based upon the results of these studies, the hematological performance of the Regent™ series should be at least equivalent to the performance of the Standard series. © *2000 Biomedical Engineering Society.* [S0090-6964(00)01105-X]

Keywords—Bileaflet mechanical heart valve, Hinge, Thrombosis, Laser Doppler velocimetry, Stress.

INTRODUCTION

Today the most widely implanted prosthetic valve design is the mechanical bileaflet. However, recent clinical data suggest that despite similar forward flow characteristics, some designs are more prone to thromboembolic episodes than others.[1] The proper functioning of the leaflets of a bileaflet mechanical heart valve requires the use of a hinge mechanism. However, the implications of this requirement have received comparatively little attention given the structural significance of the mechanism. Vallana *et al.*[13] have pointed out that the hinge design directly affects the durability of the valve, as well as its functionality and potential for thrombus formation. In particular, good washout of the hinge region is critical to reliable operation of the bileaflet mechanical heart valve, as the small characteristic dimensions and complex geometries of the confined hinge regions can provide an ideal location for thrombus formation.

Recent studies of the unacceptably high thrombosis rates of the Medtronic Parallel™ (MP) bileaflet mechanical heart valve have provided strong evidence attesting to the importance of hinge design in the overall clinical performance of a bileaflet valve.[5,6,8,11] The hinge design of the MP™ valve consisted of two cylindrical projections on the leaflet which rotated with the leaflet inside an angled hinge recess in the valve housing. The four hinge recesses were machined into the housing near the flat surface on the inflow side of the valve. In the previously cited studies,[6,8,11] the flow through the hinge of this valve was found to be dominated by unsteadiness, vortical structures, and multiple zones of stagnation especially within the inflow pocket. These findings were supported by limited clinical explant data which illustrated thrombus formation in the inflow pocket. One of the aforementioned studies[6] measured very high Reynolds shear stresses in the hinge, indicating the presence of very small turbulent eddies within this area. These eddies, which were shown to have the same length scale as an erythrocyte, have the potential to disperse their kinetic energy on blood cell membranes, resulting in cellular disruption or mechanical activation. Previous investigations of this valve design have also revealed that the near-field forward flow in the immediate downstream vicinity of the valve housing had the potential to develop localized area of reverse flow adjacent to the hinge regions, especially in the aortic position.[17] These unified studies suggest an additional mechanism accounting for the high thrombosis rate and poor clinical performance of the MP™ valve. It is possible that any blood elements

Address correspondence to Professor Ajit P. Yoganathan, Associate Chair, School of Biomedical Engineering, Georgia Institute of Technology, 654 Cherry Street, Atlanta, GA 30332-0535; electronic mail: ajit.yoganathan@bme.gatech.edu

which were convected through the already problematic flow fields of the hinge region may in turn have been entrapped in the separated or reverse flow regions of the near-field downstream forward flow.

In contrast to the performance of the MP™ valve, the St. Jude Medical® (SJM®) valve has presented very low long-term rates of thrombogenicity and valve-related events.[2,3] The SJM® Standard bileaflet mechanical heart valve was introduced for clinical use in the United States in 1977. The hinge design of this valve consists of a semicircular projection on the leaflet, called the ear, which mates to a similarly shaped recess in the valve housing. The four hinge recesses are machined into two protrusions called pivot guards that project from the inflow side of the valve. Recently the SJM® Standard series has undergone several innovations. The Hemodynamic Plus™ (HP) series was introduced in 1993 and included a sewing cuff modification which achieved a larger effective orifice area compared to the SJM® Standard valve, with an equivalent valve annulus diameter. The carbon for the HP™ valve was identical to the carbon used for the SJM Standard valve. The hemodynamic performance of the SJM® HP™ series is equivalent to that of the next size larger SJM® Standard.[9] The new SJM® Regent™ series is a modification of the currently marketed SJM® HP™ series and is now being used in clinical trials. The SJM® Regent™ valve includes an increase in the orifice dimensions over the SJM® HP™ valve with a modification of the outside geometry of the orifice housing to preserve mechanical integrity. The hinge dimensions of the Regent™ valve were kept identical to those of the SJM® Standard valve.

The purpose of this present study was to evaluate the hinge, near-hinge, and near-field forward flow dynamics of the SJM® Regent™ size 23 mm bileaflet mechanical heart valve. These studies were conducted with the primary goal of elucidating the flow patterns that are created within these regions in an attempt to obtain an improved understanding of how the design of the SJM® valve has contributed to its successful clinical record.

METHODS

Valve Models

In order to gain optical access into the hinge mechanism, St. Jude Medical® provided a 23 mm Regent™ valve model with clear housing. The leaflets were made of Delrin and the dimensions and tolerances of the clear valve were identical to those of a clinical quality SJM® Regent™ valve. The inner diameter and leaflet flat-to-flat dimensions were 0.843 and 0.752 in., respectively. The downstream near-field studies were conducted using a clinical quality 23 mm Regent™ pyrolytic carbon valve.

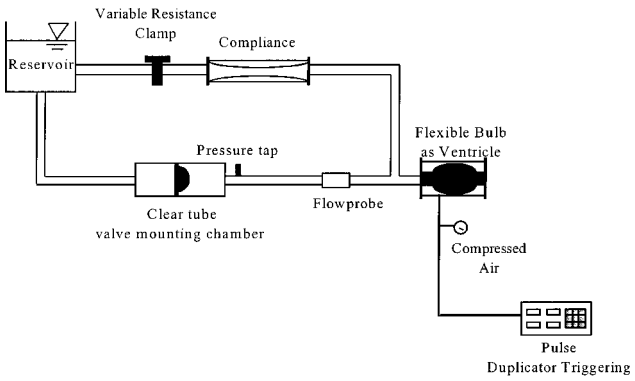

FIGURE 1. Pulsatile flow loop used for mitral hinge flow studies.

Flow Conditions

All studies were conducted in the Georgia Tech left heart pulse duplicator under a cardiac output of 5 l/min and heart rate of 70 beats/min. For the hinge flow studies, the valve model was mounted in the mitral position to simulate the harshest hinge flow and leakage conditions set up by a 135 mm Hg peak left ventricular pressure. A schematic of this flow loop is illustrated in Fig. 1. For the downstream forward flow studies, the carbon valve was placed in the aortic position to simulate the harshest near-field conditions, where the bulk-flow Reynolds number may transition into the turbulent regime. For these studies, the aortic pressure was 140/80 mm Hg and the peak systolic flow rate was 30 l/min. The mitral flow and pressure wave forms have been previously characterized[7] as have both the aortic flow loop and wave forms.[7] Flow rates were measured with an ultrasonic flow meter (Model T108, Transonic Systems Incorporated, NY) and relevant chamber pressures were measured with a physiologic pressure transducer (model P23-ID, Gould-Statham Instruments, CA). The working fluid for the studies was a solution of 79% saturated aqueous sodium iodide, 20% glycerin, and 1% water by volume. This fluid had a kinematic viscosity of 3.5 cSt to match that of blood at high shear rates. The refractive index of the fluid was adjusted incrementally to match that of the clear surfaces of the valve chambers, thereby eliminating optical distortion due to changes in refractive index. Silicon carbide particles (TSI Incorporated, MN) with a nominal diameter of 2.5 μm were used to seed the flow.

Data Acquisition

A three-component, coincident, fiber-optic laser Doppler velocimetry (LDV) system (Aerometrics Incorporated, CA) was used to obtain two-component velocity measurements within the hinge regions of the Regent™ clear valve model. Because of the additional optical de-

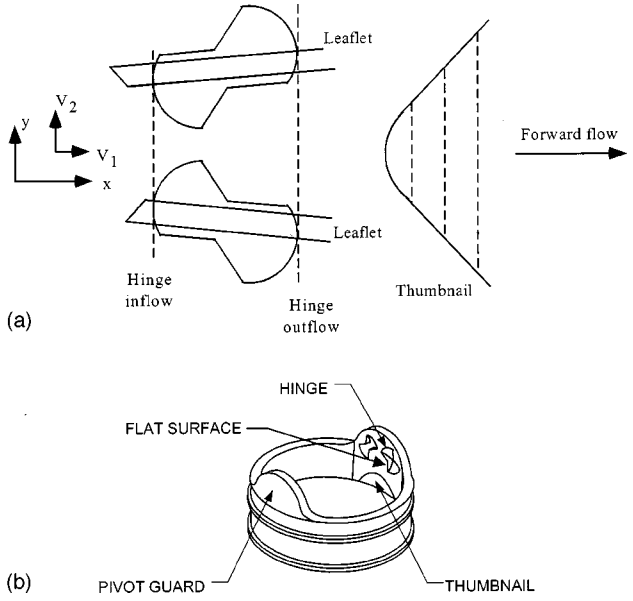

FIGURE 2. (a) Representative top view of LDV near-hinge regions. (b) Perspective view of hinge and thumbnail.

gree of freedom allowed in the near-field study, three-component velocity measurements were obtained in the downstream region of the Regent™ carbon valve. In this system, a 4 W argon-ion laser was coupled to a fiber drive unit which allowed for color separation of the primary beam. The resulting green (514.5-nm-wavelength) and blue (488-nm-wavelength) beams were used for the hinge flow measurements and the additional violet (476.5 nm wavelength) was used for the third component in the three-component measurements. A 100 mm focal length lens was coupled to the optics train to produce an ellipsoidal measurement volume with minor and major axes of approximately 21 μm$\times$140 μm.

The Doppler signals in the flow fields were processed with fast Fourier transform-based real-time signal analyzers. A commercial software package (DATAVIEW V. 0.84, Aerometrics, Inc., CA) was used to acquire data and to control both the signal analyzers and the photomultiplier hardware. A resettable clock and three-channel analog-to-digital converter were interfaced to the pulse duplicator to synchronize the acquired velocity measurements with the flow and pressure wave forms. Approximately 8000 measurements were acquired for each spatial location.

Selection of Interrogation Sites

Figure 2(A) shows a top view of the near-hinge regions of interest for the 23 Regent™ valve. These regions included a plane across the inflow edge of the hinge recesses, a plane across the outflow edge, and three planes within the thumbnail, which is a region of slight expansion that is machined into the housing of the SJM® valve and is illustrated in the perspective view of Figure 2(B). The measurements in the planes in Fig. 2 were obtained at a distance of 500 μm, 1 mm, and 3 mm below the level of the flat housing surface. Figure 3 shows a top view of a hinge illustrating representative measurement sites in the inflow and outflow hinge pockets. The measurements at the sites in Fig. 3 were obtained at the level of the flat housing surface [as depicted in Fig. 2(B)] and at distances of 195, 390, and 585 μm above the flat; these elevational views are illustrated in Fig. 4. Figure 5 shows a downstream view of the near-field region of interest. The measurement plane was positioned 1 mm downstream of the tips of the fully open leaflets and encompassed slightly over one quarter of the cross section of the aortic root.

Data Reduction

At each measurement site, the sample record was divided into a number of bins in order to decompose the pulsatile flow data into a series of discrete time intervals. Throughout these studies, a bin width of 20 ms was used. Since 8000 measurements were acquired, an average of just over 180 measurements were used for each reduction. Baldwin *et al.*[3] have shown that the statistics of mean velocity and Reynolds stress begin to converge for data set sizes of 100 measurements or greater. The calculation of the turbulent fluid stresses was accomplished using a simple decomposition technique which separated the mean-flow velocity from the fluctuating velocities within each time bin. The maximum values of the Reynolds shear stresses (mRSS) in the hinge flow fields were determined according to the formulation pub-

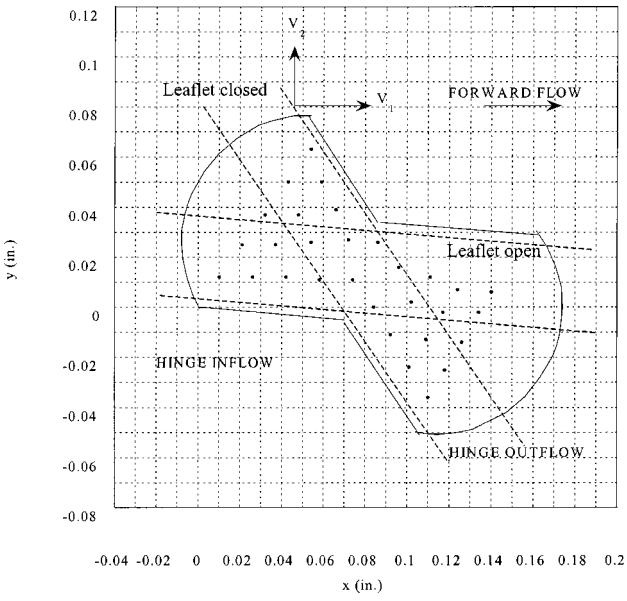

FIGURE 3. Representative top view of LDV hinge flow sites.

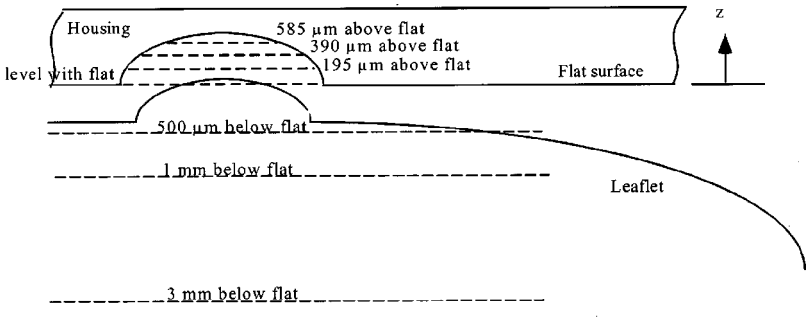

FIGURE 4. Elevational view of LDV measurement sites.

lished by Baldwin *et al.*[3] The acquired velocity data were animated in time in order to facilitate visualization of the experimental flow fields as per the automated procedure published by Healy *et al.*[10]

RESULTS

For the hinge flow studies, the results are presented in the form of color images which illustrate the flow fields at specific instances during the cardiac cycle. The arrows in the figures point in the direction of the mean-velocity vectors and are color coded as indicated in the figure legends (units m/s); their length is proportional to velocity magnitude. In each color picture, forward flow is from left to right and the orientation is as given in Figs. 2 and 3. For the near-field downstream studies, velocity profiles at selected locations of interest are presented, followed by a depiction of the peak systolic flow field throughout the quarter plane. Because the results are most readily amenable to frame-by-frame viewing in an animation sequence on a color monitor, the presentation in this paper has been limited to only the most prominent features of the respective flow fields.

23 Regent™ Mitral Hinge Flow Fields

Figures 6(A)–6(C) depict the hinge flow fields at midacceleration, peak diastole, and midsystole at the level of the flat. There were two prominent forward flow features noted [Figs. 6(A) and 6(B)]. First was the establishment of a rotating structure in the inflow hinge pocket, which was created by the confining effect of the leaflet ear upon the entering flow. The velocities in this structure were on the order of 0.10 m/s. The second prominent forward flow feature was the parallel flow through the outflow hinge pocket, where velocities ranged from 0.20 to 0.30 m/s. At midsystole, the rotating structure which was present during forward flow was abolished as the leakage jet traveled through the hinge and exited through the inflow pocket. In the inflow pocket, the leakage velocity reached 0.72 m/s and the mRSS reached 700 dyn/cm^2.

At the 195 μm elevation, the velocity field at midacceleration was nearly identical to that seen at the level of the flat, with the presence of the same rotating structure in the inflow hinge pocket. Figure 7(A) shows the velocity field at peak diastole, where the rotating inflow structure became more disturbed as the entering accelerating flow became confined between the leaflet ear and the wall of the hinge recess. By midsystole [Fig. 7(B)], a smaller region of backflow than that present at the flat was observed. At the 390 μm elevation [Fig. 7(C)], the leakage velocity reached 1.5 m/s and the mRSS reached 1000 dyn/cm^2.

23 Regent™ Mitral Hinge Inflow, Outflow, and Thumbnail Flow Fields

In the regions spanning the inflow, outflow, and thumbnail zones, the dominant flow fields features were in the forward flow phase. Figure 8 shows the peak diastolic velocity field along the hinge inflow, outflow, and thumbnail regions 1 mm below the flat. The prominent forward flow feature was the skewing of the central diastolic jet as it entered the thumbnail region and detached from the angulated housing surface, resulting in the formation of two recirculation regions. The peak central diastolic jet velocity magnitude was 1.0 m/s. The mRSS reached 650 dyn/cm^2 near the boundaries of the recirculation regions as the lateral jets penetrated the

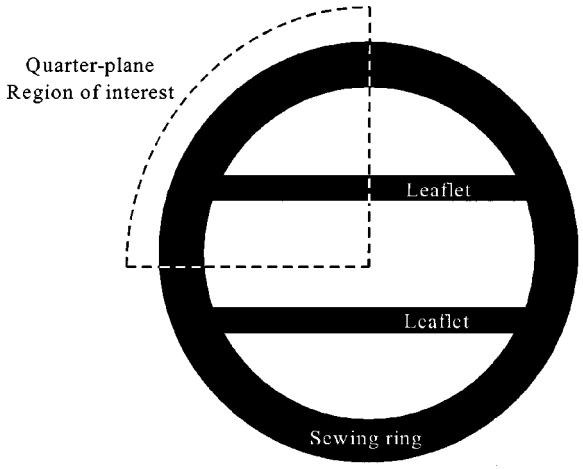

FIGURE 5. Downstream view of near-field region of interest.

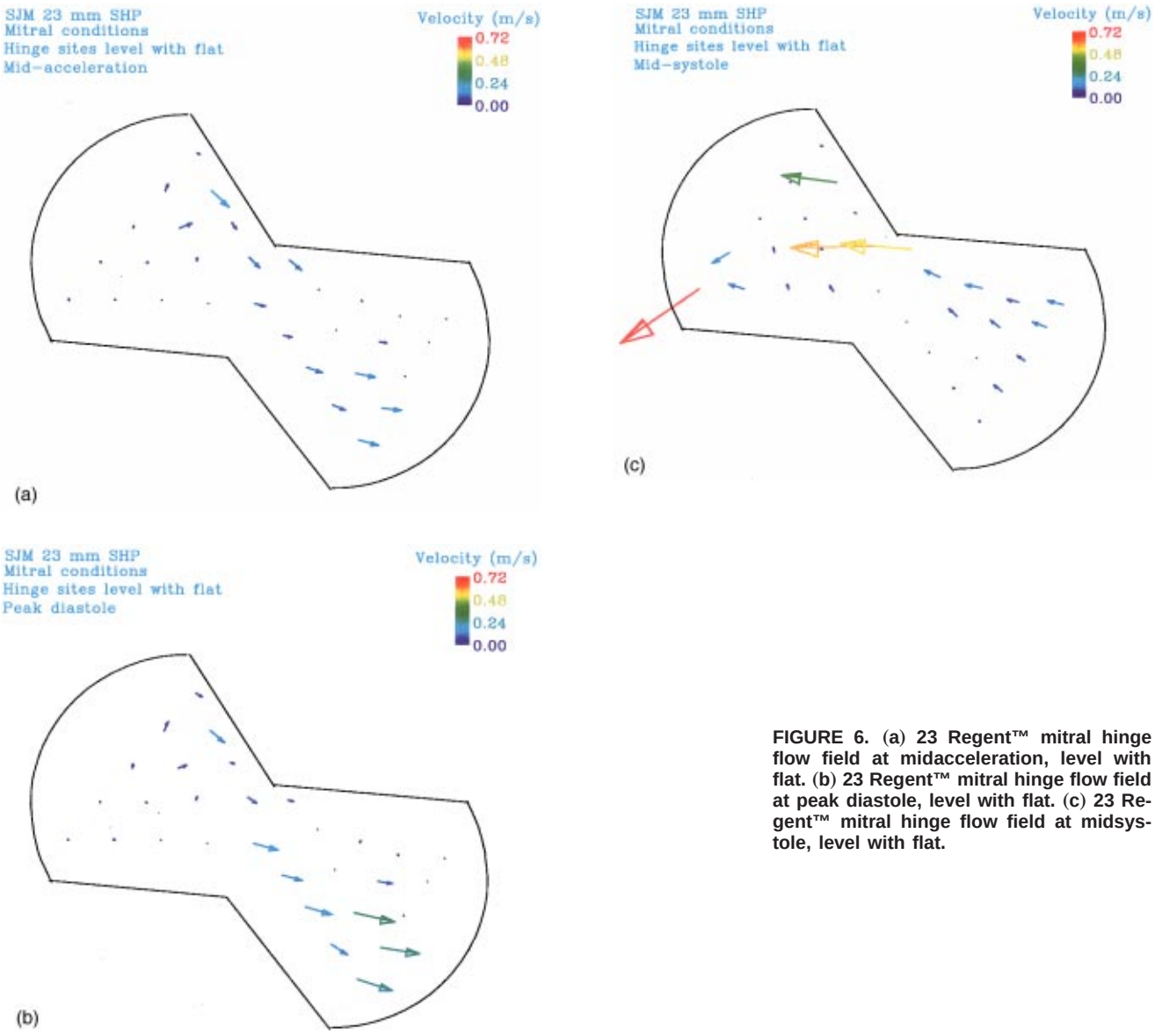

FIGURE 6. (a) 23 Regent™ mitral hinge flow field at midacceleration, level with flat. (b) 23 Regent™ mitral hinge flow field at peak diastole, level with flat. (c) 23 Regent™ mitral hinge flow field at midsystole, level with flat.

edges of the thumbnail region. These results were characteristic of the forward flow fields at the remaining elevations below the flat. At all elevations that were interrogated, regions of separated flow remained in the thumbnail region.

23 Regent™ Aortic Near-Field Forward Flow

Velocity profiles 1 mm distal to the open valve leaflets are shown in Figs. 9(A)–9(C). Axial velocity profiles along the horizontal centerline of the valve chamber are shown in Fig. 9(A). The central orifice jet was present along this profile throughout forward flow. This jet was roughly parabolic in shape, and had a peak velocity of approximately 1.7 m/s. Figure 9(B) shows axial velocity profiles 6 mm above the horizontal centerline of the valve chamber. These profiles were taken immediately distal to the lateral orifice of the valve; the single jet shown by all of these profiles is the lateral orifice jet. This jet reached a peak axial velocity of 1.8 m/s within this profile, and had a pluglike shape during most of systole. Axial velocity profiles along the vertical centerline of the valve chamber are shown in Fig. 9(C). Both the central and lateral orifice jets can be seen in this profile. The axial velocity of the central orifice jet reached a magnitude of 1.7 m/s within this profile, while that of the lateral orifice jet was as high as 2.0 m/s. The central orifice jet was parabolic in shape, while the lateral orifice jet had a more pluglike appearance.

Figure 10 shows the peak systolic velocity vectors, color coded by mRSS, over the entire measurement area.

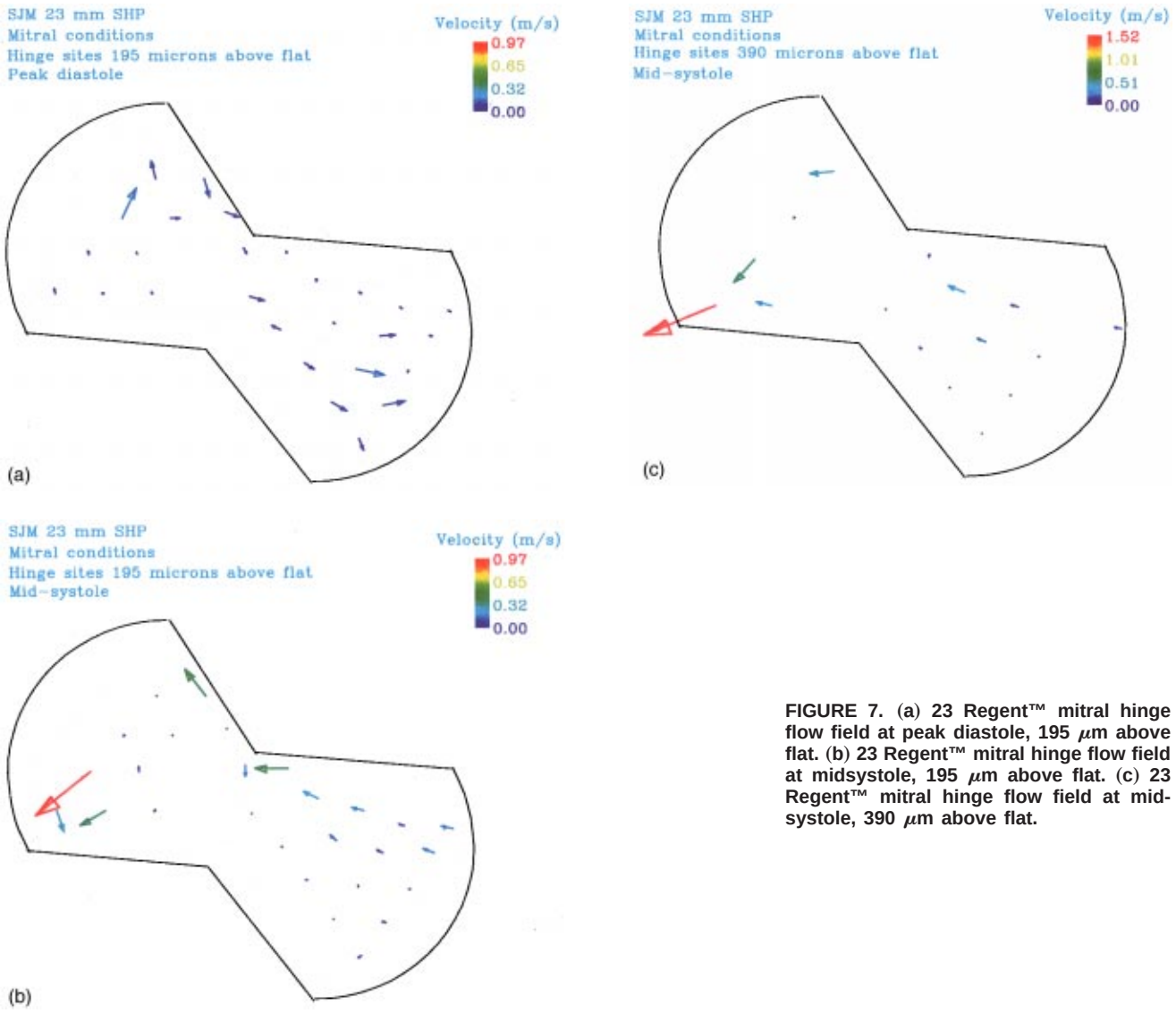

FIGURE 7. (a) 23 Regent™ mitral hinge flow field at peak diastole, 195 μm above flat. (b) 23 Regent™ mitral hinge flow field at midsystole, 195 μm above flat. (c) 23 Regent™ mitral hinge flow field at midsystole, 390 μm above flat.

Figure 10 clearly shows that the lateral orifice jet was wider and faster than the central orifice jet. Flow from the central orifice jet expanded in the direction parallel to the valve leaflets at the axial location of these measurements. Secondary flow patterns within the aortic sinus, adjacent to the hinge region, were directed from the central orifice jet outward. It is of interest to note that the secondary flow region adjacent to the hinge is immediately downstream of, and in the same radial-circumferential position as, the region of skewed flow in the thumbnail shown in Fig. 8. Relatively large values of mRSS, between 900 and 1100 dyn/cm^2, also occurred along the edges of the central and lateral orifice jets. The mRSS levels were smaller, less than 200 dyn/cm^2, within the middle of the central and lateral orifice jets and within the recirculating flow of the aortic sinus.

DISCUSSION

SJM® Regent™ Hinge Flow

The flow fields within the hinge regions of the SJM® Regent™ valve were characterized by a dynamic washout flow pattern which restricted the persistence of separated flow and stagnation zones. During systole, the highest leakage jet velocities and mRSS levels tended to occur in the regions where the leaflet impacted the hinge walls during valve closure. These measurements revealed that a strong backflow jet was created during the leakage flow phase [Figs. 6(C), 7(B), and 7(C)]; in the *in vivo* case, this jet washout may serve to keep the hinge region cleared of any deposited blood elements or pooled coagulative factors. Active leaflet motion through the hinge recesses is thus a contributing factor to the established

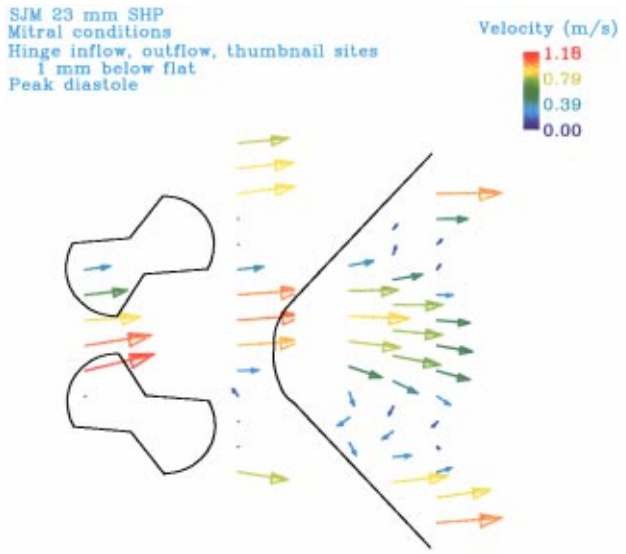

FIGURE 8. 23 Regent™ mitral hinge inflow, outflow, and thumbnail flow fields at peak diastole, 1 mm below flat.

clinical success of the similarly designed hinge of the SJM® Standard series; therefore, it would also be expected to contribute to at least an equivalent success rate for the Regent™ series.

These studies also suggest that the actual shape of the hinge mechanism influences the levels of turbulence and/or unsteadiness generated inside the hinge region, which is in essence the origin of the leakage jet. In a previous study of the MP™ hinge region[6] conducted in our laboratory, the largest mRSS was measured in the inflow region of the hinge as the backflow jet was accelerated through the narrow gap between the leaflet pivot and housing wall. For purposes of comparison, selected regions in the inflow pocket of the Regent™ valve were interrogated at what was determined to be a similar location (585 μm above the flat datum). The largest mRSS (2600 dyn/cm^2) in the Regent™ hinge was measured at this elevation and is shown in Fig. 11 for comparison with the corresponding MP™ hinge data. These results suggest that the highest levels of turbulence and/or unsteadiness in the hinge regions are generated in the backflow jet, in a confined region bounded by the leaflet pivot and the flow lumen surface of the hinge recess. One possible explanation for the higher mRSS levels in the MP™ hinge is the presence of the sharp corners and angled inflow and outflow ramps in its hinge recess. As a leakage jet flows through these abrupt changes in geometry in the MP™ hinge, there is a strong likelihood of jet detachment and/or direct impact against the corner of the inflow ramp, both of which would lead to the formation of stagnation sites and possible regions of turbulence. Indeed, the lack of strong backflow through the inflow pocket of the MP™ hinge allowed a

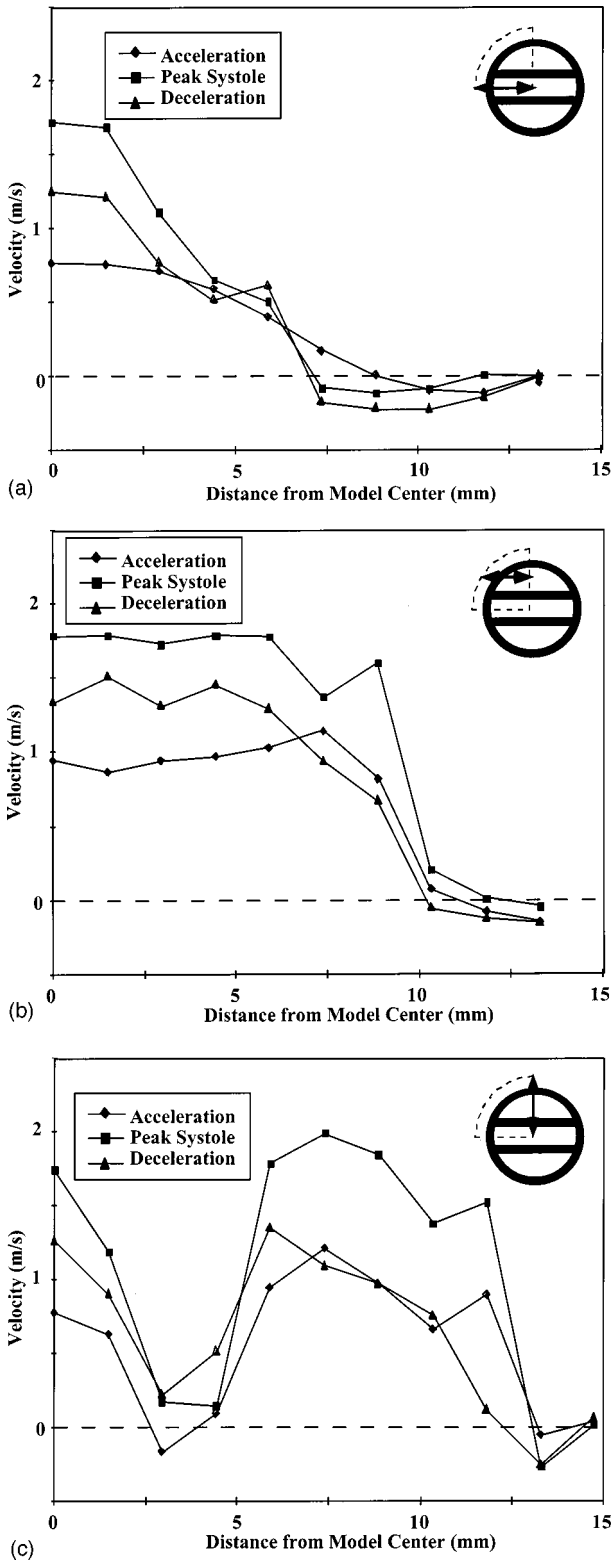

FIGURE 9. (a) 23 Regent™ velocity profiles along centerline, parallel to valve leaflets, aortic position. (b) 23 Regent™ velocity profiles 6 mm above centerline, parallel to valve leaflets, aortic position. (c) 23 Regent™ velocity profiles along centerline, perpendicular to valve leaflets, aortic position.

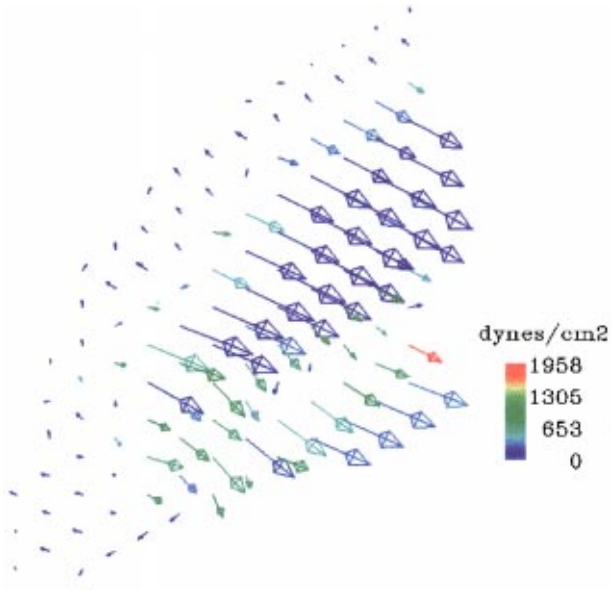

FIGURE 10. 23 Regent™ peak systolic velocity field, color coded by mRSS, aortic position.

rotating inflow structure to persist throughout the entire cardiac cycle. In contrast, the streamlined, curved profile of the SJM® Regent™ hinge recess provides a more gradual change in geometry. Correspondingly, a leakage jet flowing through the SJM® Regent™ hinge design is more likely to follow the contour of the inside surface, resulting in fewer regions of flow separation and turbulence. As a result of the strong washout, the forward flow rotating inflow structure in the Regent™ hinge was abolished by the backflow jet and did not persist beyond the forward flow phase.

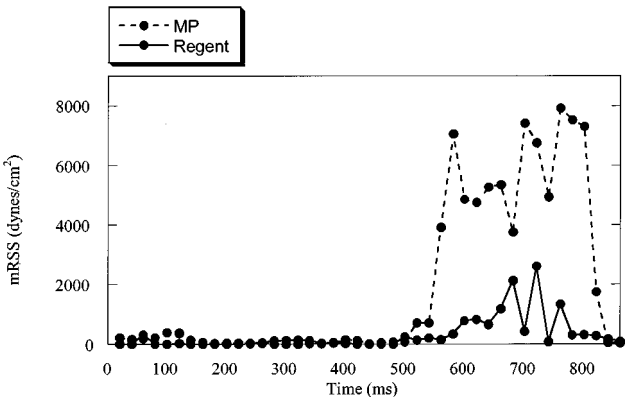

FIGURE 11. Temporal behavior of highest mRSS levels measured in Medtronic Parallel™ and St. Jude Medical® Regent™ hinge regions.

23 Regent™ Near-Field Forward Flow

The axial velocity profiles measured distal to this valve were similar to those observed in LDV studies distal to other bileaflet valves.[4,14,16] The results of these previous studies depict the central and lateral orifice jets separated by a velocity defect created by the valve leaflet. In these previous studies, however, the lateral and central orifice jets were very similar in width in a direction perpendicular to the valve leaflets. In this study, the width of the lateral orifice jet was greater than the width of the central orifice jet in this direction. This increase in width of the lateral orifice jet relative to the central orifice jet is a result of design differences between the 23 Regent™ and previous bileaflet valves.

The difference in jet widths may explain the larger velocities of the lateral orifice jet relative to those of the central orifice jet. Viscous effects were more prevalent in the smaller central orifice of this valve than the relatively wide lateral orifice. The Reynolds number of the central orifice jet, calculated using the area-averaged velocity during peak systole and the hydraulic diameter of the central orifice, was approximately 2000. However, the Reynolds number of the lateral orifice jet, calculated using corresponding values for the lateral orifice, was approximately 7000. Since the Reynolds number is a measure of the ratio of inertial forces to viscous forces, the central orifice imposes more viscous resistance to flow than the lateral orifice. The increased resistance to flow of the central orifice may be responsible for the relatively small velocity magnitudes and narrow width of the central orifice jet in a direction parallel to the valve leaflet.

The largest shear rate found in this study was localized along the edges of the lateral orifice jet. The magnitude of this shear rate was 1150 s^{-1}, corresponding to a laminar shear stress of 36 dyn/cm^2 in blood. Stresses of this magnitude for short time periods have been shown to have little effect on hemolysis and platelet activation *in vitro*.[12,15] However, the mRSS levels in the downstream near field were one to two orders of magnitude higher than the laminar shear stresses. The elevated mRSS values distal to the mating surface of the leaflet and the housing are likely a result of the complex geometry created by this intersection. The magnitudes of these mRSS levels are comparable to, but slightly less than, the magnitudes of Reynolds stresses measured distal to bileaflet valves in previous studies.[4,12,16] Other regions of elevated mRSS included the edges of the central and lateral orifice jets. This finding would be expected, as turbulent eddies can efficiently extract energy from the mean flow in the presence of large velocity gradients, such as those representative of the jets in this study. However, because the Regent™ valve offers an increase in orifice area over previous valve designs of the same

size and general design, there will likely be less kinetic energy to dissipate through turbulence as blood elements are accelerated in forward flow through the Regent™ valve.

CONCLUSIONS

The LDV measurements conducted in the hinge and near-field downstream regions of the SJM® Regent™ valve have provided a detailed depiction of the flow patterns associated with this valve design. The active leaflet motion through the SJM® Regent™ hinge and its streamlined hinge profile are important design features which should contribute to a low incidence of thromboembolism with this valve design. However, as with all valves today, there are still areas which may be vulnerable to thrombus formation due to the local fluid mechanics. These regions include (i) the thumbnail, where a skewed forward flow jet bounded by two recirculation zones did not completely wash the expanse of the thumbnail; and (ii) the near-field region immediately downstream of the thumbnail, where flow separation and secondary flows were observed. The interaction of the thumbnail flow and adjacent near-field flow are expected to be critical in allowing for adequate convection of blood elements through the valve while preventing entrapment and/or activation of these elements. Based on the results of these studies, we expect the SJM® Regent™ series to perform at least as well as the SJM® Standard series. The findings of these studies are intended to be viewed as supplementary data which should be considered together with other performance criteria, such as satisfactory and well-established structural durability and clinical histories.

ACKNOWLEDGMENTS

This study was funded by a research contract with St. Jude Medical® Inc. Partial funding was also provided by a grant through the Georgia Affiliate of the American Heart Association.

REFERENCES

[1] Akins, C. Results with mechanical cardiac valvular prostheses. *Ann. Thorac. Surg.* 60:1836–1844, 1995.

[2] Arom, K., R. Emery, B. Petersen, and D. Radosevich. St. Jude Medical® valve prothesis: Health status of the patient after 15 years. *Ann. Thorac. Cardiovasc. Surg.* 2:43–49, 1996.

[3] Baldwin, J., S. Deutch, D. Geselowitz, and J. Tarbell, Estimation of Reynolds stresses within the Penn State left ventricular assist device. *ASAIO Trans.* 36:M274–M278, 1990.

[4] Barbaro, V., M. Grigioni, C. Daniele, G. D'Aveio, and G. Boccanera. 19mm sized bileaflet valve prostheses' flow field investigated by bidimensional laser Doppler anemometry. *Int. J. Artif. Organs* 20:622–628, 1997.

[5] Baudet, E., V. Puel, J. McBride, J. Grimaud, F. Roques, F. Clerc, X. Rogues, and N. Laborde. Long-term results of valve replacement with the St. Jude Medical® prosthesis. *J. Thorac. Cardiovasc. Surg.* 109:858–870, 1995.

[6] Ellis, J., T. Healy, A. Fontaine, R. Saxena, and A. Yoganathan. Velocity measurements and flow patterns within the hinge region of a Medtronic Parallel™ bileaflet mechanical heart valve with clear housing. *J. Heart Valve Disease* 5:591–599, 1996.

[7] Ellis, J., T. Healy, A. Fontaine, M. Weston, C. Jarret, R. Saxena, and A. Yoganathan. An *in vitro* investigation of the retrograde flow fields of two bileaflet mechanical heart valves. *J. Heart Valve Disease* 5:600–606, 1996.

[8] Gross, J., M. Shu, F. Dai, J. Ellis, and A. Yoganathan, A microstructural flow analysis within a bileaflet mechanical heart valve hinge. *J. Heart Valve Disease* 5:581–590, 1996.

[9] Hayashida, N., T. Isomura, K. Hisatomi, T. Sato, H. Maruyama, K. Kosuga, and A. Shigeaki. Hemodynamic performance of the St. Jude Medical Hemodynamic Plus Valve. *Artif. Organs* 21:916–921, 1997.

[10] Healy, T., J. Ellis, A. Fontaine, C. Jarrett, and A. Yoganathan. An automated method for analysis and visualization of laser Doppler velocimetry data. *Ann. Biomed. Eng.* 25:335–343, 1997.

[11] Healy, T., A. Fontaine, J. Ellis, S. Walton, and A. Yoganathan. Visualization of the hinge flow in a 5:1 scaled model of the Medtronic Parallel™ bileaflet heart valve prosthesis. *Exp. Fluids* 25:512–518, 1998.

[12] Sallam, A. and N. Hwang. Human red blood cell hemolysis in a turbulent shear flow: Contribution of Reynolds stresses. *Biorheology* 21:783–797, 1984.

[13] Vallana, F., S. Rinaldi, P. Galetti, A. Nguyen, and A. Piwnica. Pivot design in bileaflet valves. *ASAIO J.* 38:M600–M606, 1992.

[14] Walker, P. and A. Yoganathan. *In vitro* pulsatile hemodynamics of five mechanical aortic heart valve prostheses. *Eur. J. Cardiothorac. Surg.* 6:S113–S123, 1992.

[15] Wurzinger, L., P. Blasberg, and H. Schmid-Schonbein. Towards a concept of thrombosis in accelerated flow: Rheology, fluid dynamics, and biochemistry. *Biorheology* 22:437–449, 1985.

[16] Yoganathan, A., H. Sung, Y. Woo, and M. Jones, *In vitro* velocity and turbulence measurements in the vicinity of three new mechanical aortic heart valve prostheses: Bjork–Shiley Monostrut, Omni-Carbon, and Duromedics. *J. Thorac. Cardiovasc. Surg.* 95:929–939, 1988.

[17] Yoganathan, A., A. Fontaine, J. Ellis, and T. Healy. Forward flow characteristics of a 27 mm Medtronic Parallel bileaflet aortic valve prosthesis (abstract). Proceedings of the World Congress of the International Society for Artificial Organs, Taiwan, November 14–18, 1995.